Proliferation of Multiple Cell Types in the Skeletal Muscle Tissue Elicited by Acute p21 Suppression

Maria Grazia Biferi[1], Carmine Nicoletti[2], Germana Falcone[1,3], Eleonora MR Puggioni[1], Nunzia Passaro[1], Alessia Mazzola[1], Deborah Pajalunga[1], Germana Zaccagnini[4], Emanuele Rizzuto[5], Alberto Auricchio[6,7], Lorena Zentilin[8], Gabriele De Luca[9], Mauro Giacca[8], Fabio Martelli[4], Antonio Musio[10,11], Antonio Musarò[2,12] and Marco Crescenzi[1]

[1]Department of Cell Biology and Neurosciences, National Institute of Health, Rome, Italy; [2]Institute Pasteur Cenci-Bolognetti, DAHFMO-Unit of Histology and Medical Embryology, IIM, Sapienza University of Rome, Rome, Italy; [3]Institute of Cell Biology and Neurobiology, National Research Council, Monterotondo, Italy; [4]Molecular Cardiology Laboratory, IRCCS-Policlinico San Donato, Milan, Italy; [5]Department of Mechanical and Aerospace Engineering, IIM, Sapienza University of Rome, Rome, Italy; [6]Division of Medical Genetics, Department of Translational Medicine, "Federico II" University, Naples, Italy; [7]Telethon Institute of Genetics and Medicine, Pozzuoli, Italy; [8]Molecular Medicine Laboratory, International Centre for Genetic Engineering and Biotechnology, Trieste, Italy; [9]Department of Ematology, Oncology and Molecular Medicine, National Institute of Health, Rome, Italy; [10]Institute of Biomedical and Genetic Research, National Research Council, Pisa, Italy; [11]Tumour Institute of Tuscany, Florence, Italy; [12]Center for Life Nano Science@Sapienza, Italian Institute of Technology, Genova, Italy

Although in the last decades the molecular underpinnings of the cell cycle have been unraveled, the acquired knowledge has been rarely translated into practical applications. Here, we investigate the feasibility and safety of triggering proliferation *in vivo* by temporary suppression of the cyclin-dependent kinase inhibitor, p21. Adeno-associated virus (AAV)-mediated, acute knockdown of p21 in intact skeletal muscles elicited proliferation of multiple, otherwise quiescent cell types, notably including satellite cells. Compared with controls, p21-suppressed muscles exhibited a striking two- to threefold expansion in cellularity and increased fiber numbers by 10 days post-transduction, with no detectable inflammation. These changes partially persisted for at least 60 days, indicating that the muscles had undergone lasting modifications. Furthermore, morphological hyperplasia was accompanied by 20% increases in maximum strength and resistance to fatigue. To assess the safety of transiently suppressing p21, cells subjected to p21 knockdown *in vitro* were analyzed for γ-H2AX accumulation, DNA fragmentation, cytogenetic abnormalities, ploidy, and mutations. Moreover, the differentiation competence of p21-suppressed myoblasts was investigated. These assays confirmed that transient suppression of p21 causes no genetic damage and does not impair differentiation. Our results establish the basis for further exploring the manipulation of the cell cycle as a strategy in regenerative medicine.

Received 9 June 2014; accepted 3 February 2015; advance online publication 10 March 2015. doi:10.1038/mt.2015.27

INTRODUCTION

Regenerative medicine encompasses a variety of currently available or envisioned therapeutic approaches ranging from cell replacement therapy to *in vivo* tissue or organ regeneration.[1] Despite their largely solid biological bases, many such approaches are marred by practical hurdles, one of which is insufficient cell proliferation. Slow proliferation hampers cultivation of a variety of therapeutically relevant cell types, *e.g.*, human-derived stem cells.[2] Equally affected is regeneration of many diverse tissues *in vivo*. By way of example, cartilage, tendon, and bone require extensive periods of time to heal, often imperfectly.[3] There clearly is a widespread need for techniques to induce or accelerate cell proliferation.

The central cell cycle regulatory molecules, cyclin-dependent kinases (CDKs), are activated by the binding of cyclins and restricted by CDK inhibitors (CDKIs). CDKIs belong to either the INK4 or the Cip/Kip family.[4] The first group includes four CDKIs that selectively bind Cdk4 and Cdk6 and prevent their association with D-type cyclins. The Cip/Kip family is comprised of three members, p21 or CDKN1A, p27 or CDKN1B, and p57 or CDKN1C, which preferentially bind cyclin/Cdk complexes and have broad inhibitory abilities.[5] CDKIs are expressed at high levels in most types of nonproliferating cells and critically contribute to preserve cell cycle dormancy.[6]

We have previously found that cells can be brought back into the cell cycle from all nonproliferation states, including terminal differentiation and senescence as well as quiescence, by simply removing appropriate cell cycle inhibitors, most importantly p21.[6] Such remarkable effect is mediated by preassembled cyclin/Cdk/CDKI complexes that spontaneously acquire activity upon removal of the inhibitory molecule.[6,7] Terminally differentiated cells, though reentering the cell cycle, generally cannot be made to proliferate.[8–14] In contrast, quiescent cells readily multiply following CDKI removal, even in the absence of exogenous growth factors.[6]

In this article, we explore CDKI suppression as a means to activate or expedite the proliferation of quiescent cells *in vivo* and promote or accelerate tissue repair. We show that acute p21

The first two authors contributed equally to this work.

Correspondence: Marco Crescenzi, Departmet of Cell Biology and Neurosciences, National Institute of Health Viale Regina Elena, 299, 00161 Rome, Italy. E-mail: marco.crescenzi@iss.it

removal *in vivo* triggers different cell types to proliferate, including satellite cells, greatly but temporarily increasing the cellularity of skeletal muscle and causing striking increases in strength and endurance. Furthermore, we show that transient p21 removal causes no harm to the cells. In particular, it does not induce apoptosis, DNA damage, chromosomal aberrations, or mutations and does not affect the skeletal muscle differentiation program. Thus, at least in principle, a variety of regenerative medicine approaches might benefit from controlled CDKI removal.

RESULTS

p21 suppression elicits cell proliferation *in vivo*

Although we had previously shown that interference with p21 forcefully stimulates proliferation of cultured cells, the question remained whether it could attain similar effects *in vivo*. To address this point, we electroporated otherwise intact mouse tibialis anterior (TA) muscles with p21 or control siRNA. As early as 3 days after electroporation, large areas of the p21 siRNA-transduced muscle displayed greatly increased cellularity (**Supplementary Figure S1**). In principle, these results showed that p21 suppression is as effective *in vivo* as *in vitro* in triggering proliferation of quiescent cells. However, the induced hypercellular areas were patchy, presumably due to inhomogeneous siRNA transduction, and tissue damage from electroporation complicated the interpretation of the results.

AAV-mediated p21 siRNA elicits strong and uniform proliferation of multiple cell types

To overcome the limitations of electroporation, we explored the possibility of using adeno-associated virus (AAV) vectors to transduce the muscle tissue in a more uniform and less invasive fashion. To this end, we injected a LacZ-carrying, serotype

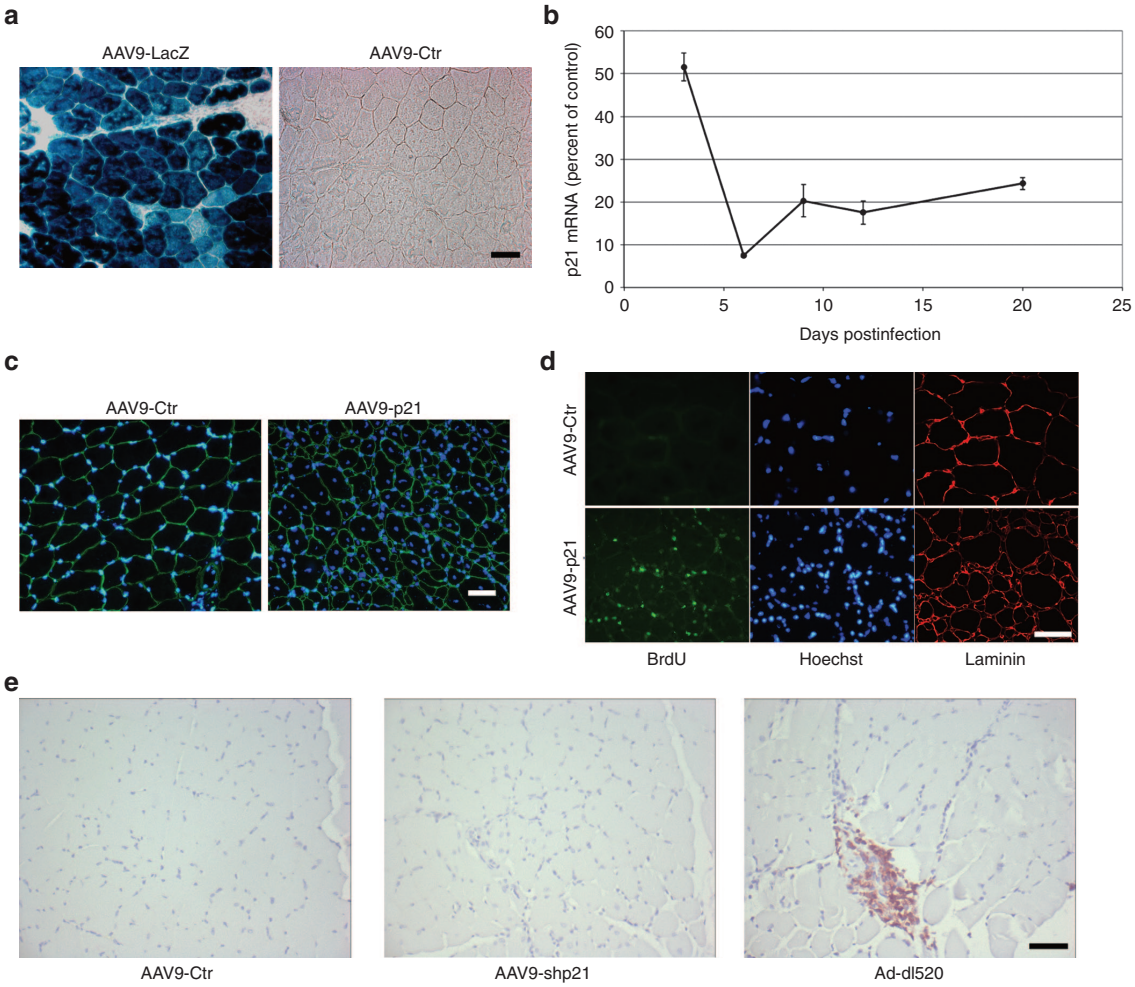

Figure 1 Effects of adeno-associated virus (AAV9)-mediated suppression of p21 in the skeletal muscle. (**a**) β-Gal expression in the right tibialis anterior (TA) muscle infected with AAV9-LacZ. In the same mouse, the contralateral muscle was injected with the control virus (AAV9-Ctr). The muscles were harvested 10 days postinfection and stained for β-Gal. (**b**) Time course analysis of p21 mRNA levels in TA muscles. Mice received intramuscular injections of AAV9-p21 or AAV9-Ctr and the muscles were harvested at 3, 6, 9, 12, 15, and 20 days postinfection. qPCR-measured p21 mRNA levels are shown as percentages of those of AAV9-Ctr-injected muscles. Values are the averages of two experiments. (**c**) Total nuclei and (**d**) BrdU incorporation in AAV9-p21 infected TA muscles 10 days postinjection. The right and left TA muscles of 3 mice were infected with the indicated viruses. Sections were stained with Hoechst 33258 (blue) and subjected to immunofluorescence for laminin (red) and BrdU (green). (**e**) Leukoocytes in AAV9-p21 infected muscles. TA muscles were infected with AAV9-p21, AAV9-Ctr, or with a replication-impaired mutant adenovirus serotype 5 (dl520). The muscles were fixed 10 days postinfection and stained with an antibody to CD45. Nuclei were counterstained with Hematoxylin. Bar: 50 μm.

9 AAV (AAV9-LacZ) vector into the TA muscles of C57BL/6 mice. In two independent experiments, 10 days postinjection, 83 and 100% of the fibers, respectively, showed intense β-gal expression throughout the length of the muscles (**Figure 1a**). This result prompted us to construct an AAV9 vector carrying four copies of a p21 shRNA under the control of the H1 PolIII promoter (AAV9-p21). TA muscles were injected with this vector or its control (AAV9-Ctr) and harvested 3–20 days after injection. To label DNA-replicating cells, some of the mice were administered 5-bromo-2′-deoxyuridine (BrdU) in drinking water for variable periods of time before sacrifice.

Effective suppression of p21 was demonstrated by quantitative polymerase chain reaction (qPCR). **Figure 1b** shows that, 6 days after injection, p21 mRNA was reduced more than 10-fold in AAV9-p21-infected muscles, compared with control muscles. A fourfold reduction persisted for at least 20 days postinjection.

Histological examination showed a progressive increase in the number of nuclei in the AAV9-p21-infected muscles, compared with AAV9-Ctr-injected or mock-treated controls. The increase became first appreciable at day 5 after injection and peaked at day 10, when the number of nuclei per tissue section, in different experiments, was two- to threefold larger in p21-suppressed muscles, compared with control ones (**Figure 1c**). Other morphological features of p21-knockdown (KD) muscles will be described later (see further below, **Figure 4** and **Supplementary Figures S4 and S5**). BrdU immunofluorescence showed that a large proportion of the nuclei in p21-suppressed muscles had undergone DNA replication (**Figure 1d**), indicating that the increased cellularity observed was due to proliferation, rather than migration of exogenous (*e.g.*, inflammatory) cells. To directly exclude that AAV injection and/or interference with p21 might cause inflammation, muscle sections were stained with a pan-leukocyte, anti-CD45 antibody, which detected white blood cells neither in control nor in p21-suppressed muscles (**Figure 1e**), consistent with the notion that AAV efficiently infects skeletal muscle with virtually no inflammatory response.[15] A replication-impaired mutant of adenovirus serotype 5, known to cause a strong inflammatory response, was used as a positive control.

To determine which cell types are induced to proliferate by p21 suppression, tissue sections were stained, 10 days postinfection, with histotype-specific antibodies (**Figure 2**; quantitation in **Supplementary Table S1**). Staining for the Pax7 transcription factor showed that satellite cells were increased more than threefold in p21-suppressed vs. control muscles (**Figure 2a**). Similarly, the number of CD31-positive (CD31$^+$), endothelial cells was 1.5-fold higher in p21-KD muscles (**Figure 2b**). In addition, staining with a connective tissue-specific monoclonal antibody[16] (BM4018, see Materials and Methods) showed this compartment to be expanded in p21-KD muscles (**Figure 2c**), suggestive of increased mesenchymal cell numbers.

Importantly, 39% of Pax7$^+$ cells were labeled by BrdU in p21-suppressed muscles, compared with 6% in controls (**Figure 2d**

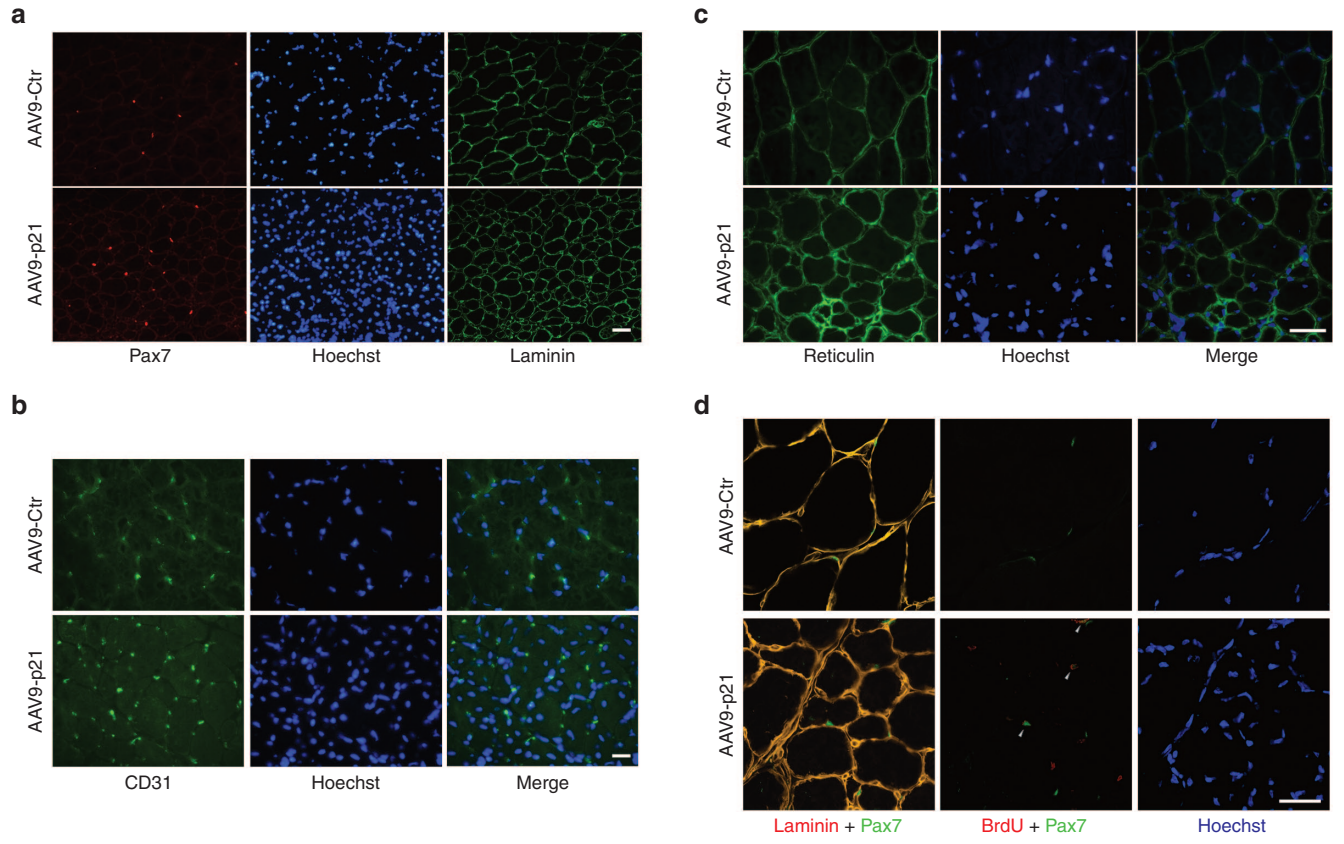

Figure 2 Analysis of cell subpopulations in adeno-associated virus (AAV)9-p21-infected tibialis anterior (TA) muscles. TA muscles infected as in Figure 1c,d were stained for the indicated antigens 10 days postinfection. Pax7$^+$ cells were counted in entire sections from each AAV9-p21- or –Ctr-infected muscle (data in **Supplementary Table S1**). All sections were also stained with Hoechst 33258 (blue). Bar: 40 µm.

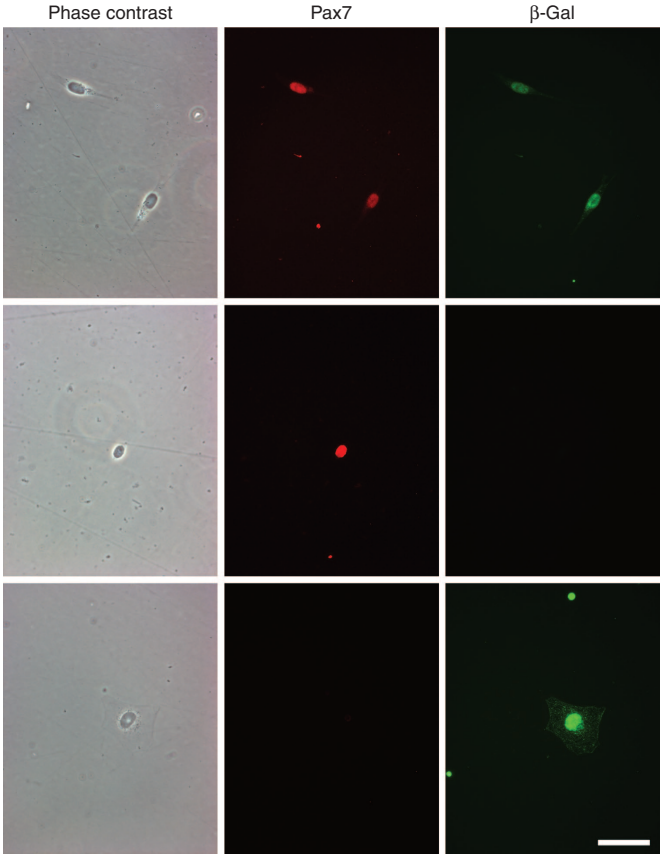

Figure 3 ***In vivo*** **satellite cell infection with adeno-associated virus (AAV)9-LacZ.** The tibialis anterior (TA) muscles of 3 mice were infected with AAV9-LacZ and were harvested 8 days postinfection. Fibers were isolated and cultured as described.[29] After 3 days in culture, cells detached from the fibers were stained for Pax7 (red) and β-Gal (green). Also shown, phase contrast pictures of the same fields. The pictures in the upper panels display double-positive cells. Staining specificity is shown in the middle and bottom panels, depicting cells positive for either Pax7 or β-Gal alone. Further examples are shown in **Supplementary Figure S3**. Bar: 40 µm.

and **Supplementary Table S1**), further demonstrating satellite cell proliferation.

To explore this relevant issue more in depth, we infected TA muscles of transgenic mice expressing NLS-LacZ under the control of a partial desmin promoter (des/NLS-LacZ). Though expressed at moderate levels in myofibers, desmin is strongly upregulated in proliferating satellite cells (SC). The des/NLS-LacZ mice display detectable β-gal activity only in the nuclei of the latter, presumably due to the incompleteness of the desmin promoter in the transgene.[17,18] These experiments showed a 10-fold increase in the number of activated SC, in AAV9-p21- versus -Ctr-infected muscles (**Supplementary Figure S2**) at day 10 postinfection. The apparent discrepancy between this large increase and the smaller one detected by direct Pax7 staining is attributable to the fact that Pax7 is downregulated upon muscle differentiation. In contrast, in des/NLS-LacZ mice, persistence of the β-Gal protein allows visualization of SC that has fused with muscle fibers (**Supplementary Figure S2**).

Altogether, these results confirm[6] that p21 KD is capable of eliciting proliferation in a broad range of cells.

p21 knockdown induces satellite cell proliferation

In view of potential applications of p21 KD in regenerative medicine, it was important to ascertain that satellite cells can be directly reactivated by p21 suppression. To this aim, we investigated whether Pax7$^+$ satellite cells can be efficiently infected by AAV9, as suggested by Dey *et al.*[19] Intact fibers were isolated from TA muscles 8 days after injection with AAV9-LacZ and put in culture. Two days later, cells migrated away from the fibers were doubly stained for β-galactosidase and Pax7 (**Figure 3** and **Supplementary Figure S3**). Of the Pax7$^+$ cells, 83.1% were β-galactosidase$^+$, showing that satellite cells are infected by AAV9 with an efficiency approaching that of muscle fibers (83–100%, see above). Together with the ability of *in vivo* p21 KD to expand Pax7$^+$ cells, induce them to incorporate BrdU, and trigger cell cycle reentry in a range of different cells,[6] these results strongly indicate that satellite cell proliferation can be induced *in vivo* by suppression of p21.

Short- and long-term morphological effects of p21 suppression in skeletal muscle

To assess the short- and long-term consequences of cell cycle reactivation, TA muscles were injected with AAV9-p21 or -Ctr vector and harvested 10, 20, 40, and 60 days thereafter. Sections representative of the entire lengths of AAV9-p21-infected muscles and controls were stained with hematoxylin and eosin (**Figure 4a**). In p21-suppressed muscles, on day 10 from injection, tissue architecture appeared somewhat disorganized. As already described, these muscles displayed diffuse hypercellularity with further, focal increases. Fiber density was augmented and fiber cross-sectional area reduced. With time and to various degrees depending on the experiment, p21-suppressed muscles tended to revert to a more normal structure (**Figure 4a**). However, a number of morphologic changes were retained, at least in part, up to 60 days postinfection, the last time point examined.

Morphometric evaluation of tissue sections showed (**Figure 4b** and **Supplementary Figure S4**) that the total number of nuclei per section remained greater, in p21-KD versus control muscles, from day 10 to 60. Similarly, the number of fibers was persistently increased by about 15% throughout the experiment, indicating that p21 suppression results in fiber neoformation. Such increase was balanced in part by a reduced fiber cross-sectional area (average, 80% of control fibers, **Figure 4b** and **Supplementary Figure S4**). However, p21-KD whole-muscle cross-sectional areas remained enlarged (from 108% at day 10 to 103% at day 60, compared with controls muscles; data not shown). While 51.9% of the p21-KD fibers displayed central nuclei at day 10, by day 60 the nuclei were mostly peripheral (p21-KD, 10.4% centronucleated fibers; control, 3.9%). This suggests that p21 suppression did not affect the maturation of the centronucleated fibers, of which nucleus peripheralization represents a morphological hallmark.[17] Trichrome staining showed that initially p21 suppression caused moderate fibrosis (blue-colored), which progressively disappeared over the next 50 days (**Supplementary Figure S5**).

p21 suppression in skeletal muscle induces transient increases in strength and endurance

We wished to evaluate whether the morphological remodeling brought about by p21 suppression is accompanied by functional

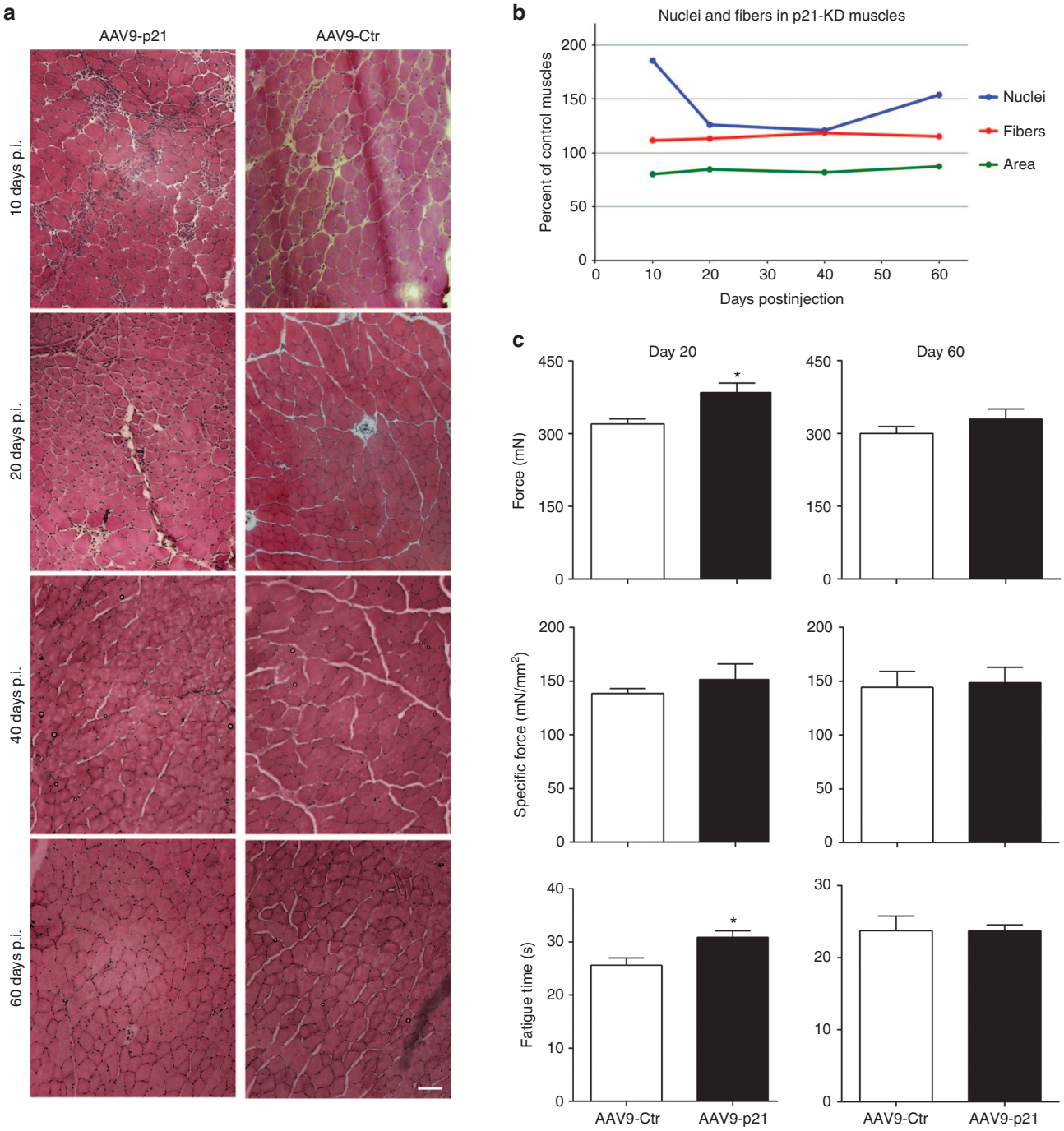

Figure 4 Effects of cell cycle reactivation in adeno-associated virus (AAV)9-p21-infected muscles. Three C57Bl/6 mice per experimental point were injected in both the right and left TA with AAV9-p21 or with AAV9-Ctr. (**a**) Sections were stained with hematoxylin and eosin at 10, 20, 40, and 60 days postinjection (p.i.). (**b**) Number of nuclei and fibers per surface unit and average fiber cross-sectional area. Sections from three different mice were scored at each time point. The results in p21-KD muscles are presented as percentages of controls. Confidence intervals for these data are shown in **Supplementary Figure S4**. (**c**) Mean ± SEM of maximum force (upper panels), specific force (middle panels) and time to fatigue (lower panels) of extensor digitorum longus muscles infected with the indicated viruses. Day 20: AAV9-p21, $n = 4$; -Ctr, $n = 6$. Day 60: -p21, $n = 6$; -Ctr, $n = 5$. Bar: 40 µm.

changes. To this aim, extensor digitorum longus (EDL) muscles were subjected to functional measurements 20 and 60 days after AAV9-p21 or AAV9-Ctr infection.

At day 20 after infection with AAV9-p21, the EDL muscles showed an average 12% increase in total weight, compared with AAV9-Ctr-infected muscles ($P < 0.05$), in keeping with their hyperplastic features. Strikingly, p21-KD muscles exhibited an average 20% increase in maximum force ($P < 0.05$, **Figure 4c**). The maximum specific force was also augmented in AAV9-p21-infected muscles, although the difference did not reach statistical significance. Furthermore, p21-KD EDLs showed a 21% increase in resistance to isotonic fatigue ($P < 0.05$, **Figure 4c**).

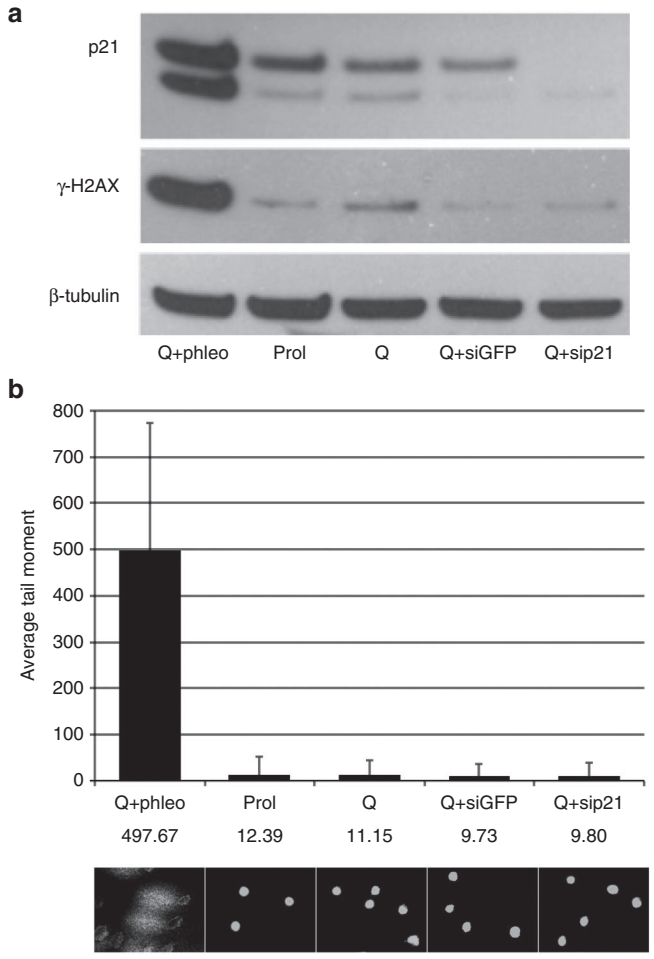

Figure 5 Assessment of DNA damage in p21-suppressed human fibroblasts. Normal, primary, human fibroblasts were rendered quiescent (Q) by culturing them in medium containing 0.1% fetal bovine serum for 96 hours. They were then subjected to RNAi for GFP (Q+siGFP, control) or p21 (Q+sip21). Proliferating cells (Prol) were added as a reference; quiescent cells treated with phleomycin (Q+phleo, 50 µg/ml for 5 hours) were included as a positive control for DNA damage. (**a**) Cells were harvested 48 hours post-treatment and analyzed by western blotting for the indicated proteins. (**b**) Cells were harvested 48 hours post-treatment and analyzed by comet assay. The graph shows average tail moment ± standard deviation; bottom pictures show examples of the analyzed nuclei. At least 65 nuclei per experimental condition were analyzed.

Sixty days after infection, the residual weight (6%, not shown) and functional differences in favor of AAV9-p21-infected muscles were no longer statistically significant.

These results show that the morphological changes generated by p21 suppression are closely paralleled by improvements in strength and endurance, indicating that the additional fibers generated as a result of cell proliferation are fully functional.

Temporary p21 suppression causes no detectable genetic or cytogenetic alterations

p21 is a major player in the DNA damage response, its main role being that of temporarily arresting damaged cells to allow repair or permanently sequestering irredeemable cells in senescence.[20] A strategy devised for regenerative medicine applications cannot afford damaging cells; thus, we subjected p21 KD cells to a variety of tests to ascertain their integrity.

To assess whether p21 suppression causes DNA breaks or allows them to accumulate unrepaired, serum-starved, quiescent human fibroblasts were reactivated by either addition of serum in the culture medium or p21 RNA interference (RNAi). **Figure 5a** shows that neither treatment caused accumulation of serine 139-phosphorylated histone H2AX (γ-H2AX), a marker of DNA double-strand (ds) breaks.[21] Fibroblasts were selected because they can be readily made quiescent by serum starvation, whereas mouse myoblasts would differentiate in the absence of growth factors. However, similar results were obtained with human myoblasts (**Supplementary Figure S6**), whose longer differentiation time allows to operationally separate quiescence from differentiation.

The possibility that p21 KD induces DNA ds breaks was also investigated using an alkaline comet assay, that directly visualizes both single-strand and ds breaks. Consistent with the lack of γ-H2AX accumulation, serum-starved human fibroblasts, reactivated by serum administration or p21 RNAi, showed no more DNA fragmentation than proliferating or quiescent cells (**Figure 5b**).

The potential for p21 KD to induce chromosomal aberrations or allow them to escape repair was investigated by cytogenetic analysis. Metaphases were prepared from proliferating normal human fibroblasts, transfected or not with p21 siRNA. The same cells, rendered quiescent by serum starvation, were reactivated by serum addition or p21 RNAi and subjected to cytogenetic analysis at the time of their first mitosis. The types and numbers of chromosomal aberrations detected in all of these conditions showed no significant differences (**Table 1**). The number of aneuploid cells also showed no meaningful changes in any of the settings investigated (**Table 1**).

To determine whether p21 ablation negatively affects cells in the longer term, quiescent fibroblasts were transfected with p21 or control siRNA and kept in culture in 0.1% fetal bovine serum (FBS) for nine days. While p21 KD cells proliferated in these conditions, control siRNA-transfected cells were reactivated by serum addition 24 hours before harvesting for metaphase preparation. Again, no significant differences were observed between p21 KD and control fibroblasts, with regard to chromosomal aberrations and ploidy (**Table 1**, long term).

Finally, the possibility that p21 KD allowed mutations to accumulate was investigated using the highly sensitive HPRT mutation assay, which measures the frequency of acquired resistance to 6-thioguanine (6-TG) in a cell population. Such resistance arises when the single functional copy of the HPRT gene on the active X chromosome acquires an inactivating mutation.

Quiescent human fibroblasts were reactivated by p21 RNAi or transfected with control siRNA. After four days in culture in the absence of serum, the cells were switched to serum-containing medium for further 5 days, then seeded in selective medium. In two independent experiments, the p21 KD cells showed a frequency of 6-TG-resistant clones indistinguishable from that of controls. UV-treated, positive-control cells showed the expected high number of mutants (**Table 2**).

Altogether, these experiments show that medium-term suppression of p21 is well tolerated by cells and does not cause DNA damage, chromosomal aberrations, or genetic mutations.

Table 1 Cytogenetic aberrations in human fibroblasts subjected to p21 RNAi

Initial proliferation state	Treatment	Percent aneuploid	Chromosomes (average ± SD)	Total aberrations/cell	Gaps/ cell	Breaks/ cell
Proliferating	—	4	45.99 ± 0.26	0.05	0.05	0
Proliferating	p21 RNAi	8	45.98 ± 0.37	0.08	0.08	0
Quiescent	p21 RNAi	2	45.99 ± 0.24	0.03	0.02	0.01
Quiescent	Fetal bovine serum	4	46.00 ± 0.20	0.03	0.02	0.01
Quiescent	Long-term p21 RNAi	6	45.97 ± 0.30	0.09	0.06	0.03
Quiescent	Long-term Ctr RNAi	7	45.98 ± 0.42	0.08	0.06	0.02

SD, standard deviation.

Table 2 Mutation frequencies in p21-suppressed and control fibroblasts

	Mutation frequency (× 10^6)	
Treatment	Experiment 1	Experiment 2
Untreated	ND	2.6
Ctr siRNA	7.4	3.5
p21 siRNA	7.0	3.3
UV	58.0	ND
Ctr siRNA + UV	ND	50.6
p21 siRNA + UV	ND	26.0

Ctr, control; ND, not done; UV, ultraviolet light (positive control).

p21 suppression does not impair the skeletal muscle differentiation program

To determine whether p21 KD might affect muscle differentiation, primary mouse myoblasts were transfected with control or p21 siRNA and induced to differentiate from 2 to 10 days after transfection. Western blotting showed that p21 was suppressed in myoblasts until 4 days from transfection (**Figure 6a**). No reduction was found in the ability of p21-suppressed cells to differentiate or fuse at any time point (**Figure 6b**,**c** and **Supplementary Figure S7**). Thus, contrary to what has been reported for constitutive, p21 KO mice,[22] acute ablation of p21 does not appreciably affect skeletal muscle differentiation *in vitro*. Indeed, *in vivo,* p21 KD-reactivated satellite cells ostensibly fuse with preexisting myofibers or form new ones (centronucleated fibers, **Figure 4**), reinforcing the conclusion that full p21 expression is not indispensable for skeletal muscle differentiation.

DISCUSSION

In this paper, we address two critical issues concerning the manipulation of the cell cycle in favor of regenerative medicine: efficacy and safety. We show that acute p21 ablation in the context of intact skeletal muscle tissue triggers multiple cell types to undergo a brief but intense proliferation burst. Furthermore, a variety of assays carried out with multiple cell types detected no genetic, chromosomal, or differentiative alterations as results of p21 suppression.

In analyzing what cell types are induced to proliferate by p21 KD, we focused our attention on satellite cells, because of their therapeutic significance. We show that these cells are efficiently infected by AAV9 and, in response to p21 suppression, incorporate BrdU *in vivo* and dramatically increase in number. Recently, it has been shown that skeletal muscle precursor cells include a slowly-proliferating, label-retaining, self-renewing subpopulation and a differentiation-committed one.[23] Proliferation of the latter subpopulation appears to be controlled by p21, while the former is largely p21-independent. On the basis of these results, cell cycle reactivation mediated by p21 KD should act mostly or exclusively on the more committed progenitor cells. Although the precise target of p21 KD is relevant to design long-term therapeutic strategies, in the present work we have not directly investigated this issue.

The hyperproliferation brought about by p21 KD spontaneously ceases within 15–20 days, though p21 mRNA remains strongly downregulated until at least 20 days postinfection (**Figure 1b**). The finding that, in p21-KD muscles, fibers are increased in number but display a smaller average cross-sectional area (**Figure 4**) might suggest that suppression of the CDKI induces proliferation without concomitant, sufficient protein synthesis. Alternatively or in addition, homeostatic mechanisms at levels above that of cell cycle control might tend to bring the muscle back to its original state, in the absence of requests (*e.g.*, overload or sustained exercise) for higher performance. In this view, such mechanisms would impinge on both trophism and proliferation. At this stage, we have no data as to the molecular bases of the spontaneous return to quiescence.

Whatever the reasons for the transience of proliferation, it results in increased absolute fiber numbers (**Figure 4b**), leading to the remarkable conclusion that at least a fraction of the additional cells produced by p21 KD generate entirely new fibers. Furthermore, despite the short duration of proliferation, most tissue changes induced by the initial burst of cell division are long-lasting. Indeed, even 60 days after p21-KD, the total number of nuclei remained increased by 67% and that of fibers by 21% (**Figure 4b**).

The current results cannot distinguish whether muscle hyperplasia is solely the effect of p21 KD on satellite cells or, rather, proliferation of interstitial cells contributes to it, perhaps by modifying satellite cell behavior. This point will be investigated by driving p21 KD with cell type-specific promoters. Irrespectively, the hyperplasia induced by p21 suppression results in striking increases in both maximum strength and resistance to fatigue. The former is a clear indication of the functionality of the supernumerary fibers induced by p21 KD. The latter is measured with a load equal to one third of maximum force, which allows each muscle to generate its maximum power. Thus, the stronger p21-KD muscles

showed reduced fatigability even while undergoing a heavier exertion than controls. This result implies an ameliorated capacity of the muscle to counteract fatigue, suggesting an increased energy reserve.

It will be of great interest to determine whether the hyperplastic response to p21 suppression can be converted into fiber hypertrophy, *e.g.*, by subjecting p21-KD muscles to overload. Even more important, future studies will try to exploit induced hyperplasia for therapeutic purposes. However, downregulation of p21, as performed in this work, is unselective, being driven by the H1 promoter. Generalized cell proliferation and deep tissue remodeling prevent a precise assessment of the benefits of p21 KD to muscle regeneration. Therapeutic approaches will need to focus on one or more specific cell types, particularly satellite cells.

Thus, the present results do not attempt to establish a therapeutic technique. Rather, they demonstrate in principle that proliferation can be effectively and safely elicited, *in vivo* as well as *in vitro*, by manipulating a single CDKI. Hence, we predict that this approach will be of great value in accelerating the healing of a variety of focal or diffuse lesions from diseases or traumas, especially in slowly self-renewing/regenerating tissues.

Using a wide range of complementary assays, we have shown that, *in vitro*, transient downregulation of p21 causes no harm to cells. Temporary modulation should be precisely the objective of future therapeutic protocols. Indeed, in regenerative medicine, any induced or accelerated proliferation is required only for a limited period of time. To avoid interference from muscle differentiation, most safety experiments have been performed with fibroblasts, rather than muscle cells. However, since the role of p21 in cell cycle control and DNA repair is not believed to be tissue specific, our results should apply to most or all histotypes. In fact, they pertain equally to *in vitro* and *in vivo* applications of p21 KD and authorize designing and experimenting with such strategies.

The ability of p21 KD to trigger strong proliferation is in apparent contrast with the largely normal phenotype of p21 knockout mice. However, it is well known that constitutive gene suppression in the course of development can often elicit compensatory responses,[24] which are less likely or less prompt in the case of acute ablations (*e.g.*, Camarda *et al.*[25]).

The finding that p21 suppression does not hinder myoblast differentiation is somewhat surprising, in light of previous results showing impaired differentiation of myogenic precursor cells and delayed regeneration of skeletal muscle in p21 knockout mice.[22] Once again, constitutive suppression[22] and short-term interference (this work) might produce different phenotypes. In any case, as already discussed, therapeutic, *in vivo* p21 suppression should

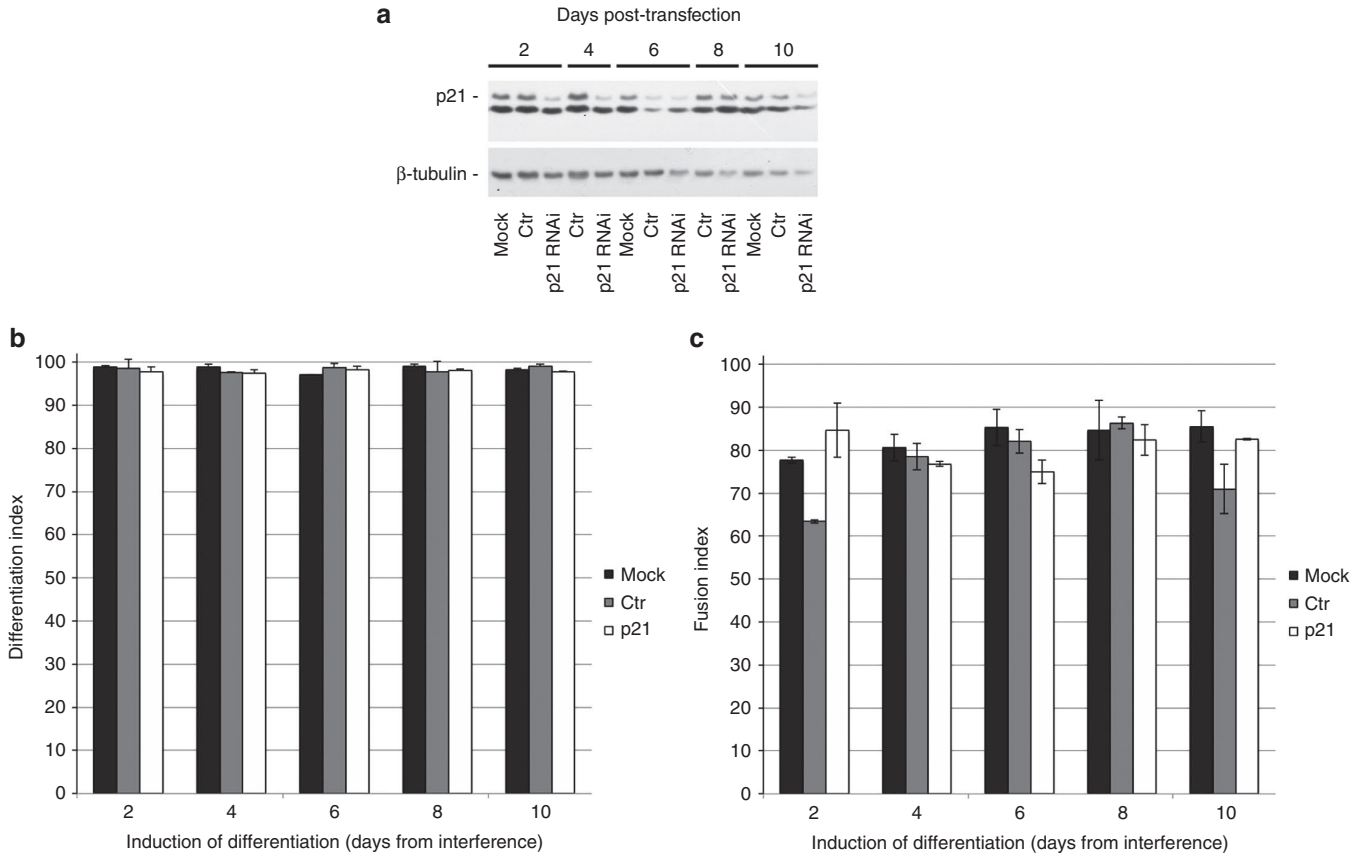

Figure 6 Effects of p21 suppression on the skeletal muscle differentiation program. Proliferating SC were transfected with siRNA to p21 or control siRNA or mock transfected. Replica cultures were induced to differentiate as indicated, from 2 to 10 days post-transfection. The cultures were fixed three days later, stained for muscle-specific myosin heavy chain (MyHC, a marker of differentiation), counterstained with Hoechst 33258, and scored. (**a**) Western blot analyses of the indicated proteins. (**b**) Differentiation index (percentage of nuclei in MyHC$^+$ cells) ± standard deviation. (**c**) Fusion index (percentage of nuclei in MyHC-positive cells with three or more nuclei) ± standard deviation. Micrographs are shown in **Supplementary Figure S7**.

be strictly limited in time. Even if temporary p21 reduction led to a momentary impairment of muscle regeneration, the amplified population of satellite cells should promptly return to normal functionality and quicken the pace of tissue repair.

MATERIALS AND METHODS

Animals,* in vivo *electroporation, and adeno-associated vectors. Animal care followed the directives of the EU (86/609/EEC). The experimental protocol was approved by the National Committee of the Italian Ministry of Health. Wild type C57Bl/6 mice were purchased from Harlan (Indianapolis, IN). TA muscles of C57Bl/6 mice were electroporated as described[26] with a siRNA to murine p21.[6] Recombinant adeno-associated viruses serotype 9 (AAV9) were produced in the laboratory of L. Zentilin and M. Giacca at the International Centre for Genetic Engineering and Biotechnology, Trieste, Italy and in the laboratory of A. Auricchio at the Telethon Institute of Genetics and Medicine, Naples, Italy. AAV9-p21 was constructed by inserting 4 copies of a shRNA to murine p21 into an AAV backbone, as previously described.[27] The antisense sequence for the shRNA to p21 is: 5′-AGCTTTT CCAAAAAGGTGATGTCCGACCTGTTCTCTCTTGAAGAACA GGTCGGACATCACCGGG-3′. The insertless AAV backbone was used as control. In some experiments, a different AAV9 vector was used, carrying a single copy of the p21 shRNA and constructed as described.[28] In these experiments, the matching control was a virus containing an shRNA to an irrelevant mRNA (rhodopsin, only expressed in retinal photoreceptors).[28] No functional differences were observed between the two sets of viruses.

For intramuscular injections, mice were anesthetized with Avertin. All infections were performed with a single injection of 50 µl of a 1.5×10^{11} vg/ml viral stock directly into the TA muscle, using a 32G needle. Satellite cell isolation from cultured fibers of AAV-LacZ infected muscles was performed as described.[29]

Immunofluorescence, histological analysis, and microscopy. For immunofluorescence procedures, cells were fixed with 4% formaldehyde for 10 minutes and permeabilized with 0.1% Triton X-100 (ICN Biomedicals, Aurora, OH) in phosphate-buffered saline. Monoclonal antibodies (MoAbs) to the following antigens were used: BrdU (Bu20a clone, Dako-Cytomation, Glostrup, Denmark); myosin heavy chain (MF20, ref. 30); γ-H2AX (05-636, Millipore (Billerica, MA)). Alexa Fluor 488- or 594-conjugated antisera to mouse immunoglobulins were obtained from Life Technologies (Carlsbad, CA). Nuclei were counterstained with Hoechst 33258 (Sigma, St. Louis, MO).

For histological stainings, TA muscles were harvested and immediately snap frozen. Eight-micrometer cryosections were fixed in 4% paraformaldehyde and processed for histological and immunofluorescence analysis. The following MoAbs and antisera (AS) were used: sheep AS to BrdU (Ab1893, Abcam, Cambridge, UK); MoAb to Pax7 (Developmental Studies Hybridoma Bank, Iowa City, IA); rabbit AS to laminin (L9393, Sigma); rabbit AS to CD31 (Ab28364, Abcam); rat MoAb to reticular fibroblasts (Pan Reticular, BM4018, Acris Antibodies, Herford, Germany). Muscle sections were also stained with hematoxylin, eosin, and Masson's trichrome (Sigma). Immunohistochemistry for CD45 (rat AS 553082 Becton Dickinson, Franklin Lakes, NJ) was carried out on formalin-fixed sections, according to previously published procedures.[31] For double Pax7/BrdU staining, the following primary antibodies were used: MoAb to Pax7 (sc81648, Santa Cruz, Dallas, TX); biotinylated sheep AS to BrdU (ab2284, Abcam). All histological evaluations were carried out on transverse sections evenly distributed throughout the length of the muscle, to avoid biases due to local inhomogeneities.

Pictures were obtained using a fluorescence microscope (Axioskop 2; Carl Zeiss MicroImaging, Oberkochen, Germany), with a 20× or 40× objective. Images were digitized with a camera (AxioCam; Carl Zeiss MicroImaging) and acquired with AxioVision 3.1 software (Carl Zeiss MicroImaging). Double Pax7/BrdU images were acquired using a Leica SPE confocal microscope with a 40× objective (Leica, Solms, Germany). Photographs were contrast enhanced by applying the brightness/contrast regulation of the Photoshop CS 8.0 software (Macintosh version, Adobe, San Jose, CA) to the whole image. Double immunofluorescence images were obtained by superimposing two single-color pictures of the same field.

***BrdU incorporation* in vitro *and* in vivo.** To assess cell cycle reactivation, quiescent cell cultures were cultured for 24 hours in the presence of 20 µmol/l BrdU (Sigma). Mice were administered 2.6 mmol/l BrdU in drinking water. This route, compared to the more commonly used intraperitoneal administration, has the advantage of sparing the animals repeated injections and of being more suitable for long-term labeling. Since the *in vivo* half-life of BrdU is less than 1 hour, oral delivery provides more uniform labeling over extended periods of time. We observed no side effects in mice given BrdU in water for up to 15 days.

RNA extraction, reverse transcription, and real-time PCR quantification. Total RNA was extracted from freshly frozen TA muscles with TRIzol Reagent (Life Technologies) according to the manufacturer's instructions. After treatment with DNase I (New England BioLabs, Ipswich, MA), RNA quality was verified by gel electrophoresis. cDNA was synthesized from RNA using the High-Capacity cDNA Reverse Transcription Kit (Life Technologies). TaqMan PCR was performed using a 7500 Fast Real-Time PCR Systems (Applied Biosystems, Waltham, MA). Amplified cDNA (60 ng) was mixed with the SensiMix II Probe reagent (Bioline, London, UK), 1 µl of p21 TaqMan Assay (Mouse p21 Mm 01303209_m1 FAM/MGB probe) and 1 µl of GAPDH TaqMan Assay (Mouse GAPDH Endogenous Control VIC/MGB probe (Life Technologies). Amplification cycles included 95 °C, 15 seconds denaturing and 60 °C, 60 seconds annealing/synthesis steps.

Cell cultures and RNAi experiments. Low-passage human primary foreskin fibroblasts (FB1329) were cultured in Dulbecco's modified Eagle's medium supplemented with 10% FBS (Life Technologies) and antibiotics (100 U/ml penicillin and 100 µg/ml streptomycin, Life Technologies). Quiescence was induced by switching confluent cultures to 0.1% FBS for 48–96 hours, depending on the experiment. Cells were considered quiescent when BrdU incorporation over 24 hours was lower than 5%. Primary myoblasts were isolated and cultured as previously described.[32] SKMC human skeletal myoblasts from a single donor were obtained from Cambrex (Rutherford, NJ).

siRNA experiments were performed following a previously described procedure.[6] Briefly, Target cells were transfected with the HiPerFect transfection reagent (Qiagen, Venlo, The Netherlands) complexed with siRNAs to p21 or control siRNA (siGENOME SMARTpool Upgrades, Dharmacon, Lafayette, CO).

Western blot analyses. Proteins were separated on gradient, 4–12% polyacrylamide gels (Invitrogen, Carlsbad, CA) and analyzed by western blotting with the following antibodies: β-tubulin (T5293, Sigma); p21 (sc-397, Santa Cruz Biotechnology); γ-H2AX (05636, Upstate, Charlottesville, VA). Peroxidase-conjugated antisera to mouse and rabbit immunoglobulins were purchased from Bio-Rad Laboratories (Hercules, CA). Western blots were developed using the LiteAblot Extended substrate (Euroclone, Pero, Italy).

Functional measurements. For functional studies, virus injections were performed into TA muscles but, as demonstrated by β-galactosidase staining and Pax7+ cell enumeration (data not shown), EDL muscles were equally infected. EDL muscles were subjected to functional measurements 20 and 60 days after AAV9-p21 or -Ctr infection. Time to peak, half relaxation time, maximum force value, and resistance to isotonic fatigue were measured as previously described.[33] In particular, time to fatigue was computed as the time each muscle was able to shorten repeatedly against a resistant load equal to one-third of its maximum force. Muscle length and weight were measured at the end of each experiment for force normalization.

Single cell gel electrophoresis (comet assay). Alkaline single cell gel electrophoresis was performed as described (ref. 34). Briefly, cell suspensions were mixed with 0.5% low melting point agarose/phosphate-buffered saline (Bio-Rad) and applied to glass microscope slides coated with 1% low melting point agarose. The gel was allowed to solidify at 4 °C, then the slides were submerged in lysis solution (2.5 mol/l NaCl, 100 mmol/l ethylenediaminetetraacetic acid (EDTA), 10 mmol/l Tris, 1% Triton X-100, 10% dimethyl sulfoxide (DMSO), pH 10) and kept at 4 °C overnight. The slides were then incubated for 20 minutes in alkaline buffer (300 mmol/l NaOH, 1 mmol/l EDTA, pH 13). Electrophoresis was performed in alkaline buffer at 300 mA for 30 minutes at room temperature. After electrophoresis, the slides were placed in neutralization buffer (0.4 mol/l Tris-NaOH, pH 7.5) for 5 minutes and then fixed in cold 100% ethanol for 5 minutes. Slides were air dried and stained with ethidium bromide, 20 μg/ml in water. Comet images were analyzed using the IAS 2000 7.0 software (Delta Sistemi, Roma, Italy). At least 50 nuclei per experimental point were analyzed. The tail moment parameter is calculated as (percentage of DNA in the tail) × (head-to-tail distance). Nuclei with apoptotic morphology (very small comet heads and extremely large tails) were excluded from analysis.

Cytogenetic analyses. Subconfluent cultures of FB1329 fibroblasts were made quiescent in 0.1% FBS-containing medium and, 48 hours later, transfected with p21 siRNA or fed 10% FBS. After 32 hours (p21 siRNA) or 23 hours (10% FBS), the cells were processed for metaphase preparation. For long-term treatments, quiescent FB1329 fibroblasts were transfected with p21 siRNA, maintained in culture in medium containing 0.1% FBS, and processed 9 days later for metaphase preparation. Twenty-four hours before metaphase preparation, cells transfected with control siRNA were fed 10% FBS to induce cell cycle reactivation. To prepare metaphase spreads, the cells were treated with 0.4 μg/ml Colcemid (Sigma) for 3 hours at 37 °C, then harvested and incubated with 75 mmol/l KCl for 30 minutes at 37 °C. Nuclei were fixed in suspension with methanol/acetic acid 3/1 and kept at 4 °C for 12 hours.[35] Chromosome preparations were Giemsa stained; ploidy and chromosomal aberrations were scored by direct microscopic examination. One hundred metaphase spreads per sample were analyzed.

HPRT gene mutation assay. The HPRT assay was applied to proliferating human primary fibroblasts and quiescent ones treated with siRNA to p21 or control siRNA. At the end of the expression period, 7×10^4 cells were seeded into 90-mm dishes in medium containing 10% FBS and 7.5 μg/ml 6-TG (Sigma). The medium was renewed after 10 days and, after 10 additional days, colonies of 6-TG-resistant cells were fixed with methanol, stained with 5% Giemsa reagent and counted. As a positive control, quiescent fibroblasts were treated with 8 joule/m^2, 254 nm UV light. Cloning efficiency was determined in medium without 6-TG, in parallel, duplicate cultures seeded at 100 cells per 60-mm dish and allowed to grow for 10 days. Colonies were then fixed, stained, and counted as above. Mutation frequency is expressed as the number of 6-TG-resistant colonies per 10^6 cells, normalized to cloning efficiency.[36]

SUPPLEMENTARY MATERIAL

Figure S1. Suppression of p21 in the skeletal muscle by electroporation of siRNA induces hypercellularity.
Figure S2. Expression of β-Gal in des/NLS-LacZ mice upon infection.
Figure S3. In vivo satellite cell infection with AAV9-LacZ.
Figure S4. Effects of cell cycle reactivation in AAV9-p21-infected muscles.
Figure S5. Masson's trichrome staining of AAV9-p21-infected muscles.
Figure S6. Assessment of DNA damage in p21-suppressed human skeletal myoblasts.
Figure S7. Effects of p21 suppression on the skeletal muscle differentiation program.
Table S1. Density of cd31$^+$ and Pax7$^+$ cells and BrdUincorporation into Pax7 cells in infected muscles.

ACKNOWLEDGMENTS

The authors thank Giulia Piaggio and Isabella Manni for generously providing access to their MITO-Luc mice, Paola Fortini for help and assistance with qPCR, Irene Bozzoni for donating the psiUx construct, Sonia Alonso-Martin for help with isolated muscle fibers, and Maurizia Caruso for helpful suggestions on Pax7 staining. This work was supported by grant no. 15715 to M.C. from the Association Francaise contre les Myopathies; grant IG11471 to A. Musio from the Associazione Italiana Ricerca sul Cancro; Advanced Grant 250124 from the European Research Council and Project PRIN 2010RNXM9C from the MIUR, Italy, to M.G.; F.M. is supported by the Ministry of Health, Italy, Telethon-Italy (grant no. GGP14092), and Cariplo Foundation (grant no. 2013-0887); A. Musarò received support from Telethon, AFM, and PRIN.

REFERENCES

1. Mason, C and Dunnill, P (2008). A brief definition of regenerative medicine. *Regen Med* **3**: 1–5.
2. Cheng, T (2004). Cell cycle inhibitors in normal and tumor stem cells. *Oncogene* **23**: 7256–7266.
3. Peng, H and Huard, J (2004). Muscle-derived stem cells for musculoskeletal tissue regeneration and repair. *Transpl Immunol* **12**: 311–319.
4. Sherr, CJ and Roberts, JM (1999). CDK inhibitors: positive and negative regulators of G1-phase progression. *Genes Dev* **13**: 1501–1512.
5. De Clercq, A and Inzé, D (2006). Cyclin-dependent kinase inhibitors in yeast, animals, and plants: a functional comparison. *Crit Rev Biochem Mol Biol* **41**: 293–313.
6. Pajalunga, D, Mazzola, A, Salzano, AM, Biferi, MG, De Luca, G and Crescenzi, M (2007). Critical requirement for cell cycle inhibitors in sustaining nonproliferative states. *J Cell Biol* **176**: 807–818.
7. Falcone, G, Mazzola, A, Michelini, F, Bossi, G, Censi, F, Biferi, MG *et al.* (2013). Cytogenetic analysis of human cells reveals specific patterns of DNA damage in replicative and oncogene-induced senescence. *Aging Cell* **12**: 312–315.
8. Feddersen, RM, Ehlenfeldt, R, Yunis, WS, Clark, HB and Orr, HT (1992). Disrupted cerebellar cortical development and progressive degeneration of Purkinje cells in SV40 T antigen transgenic mice. *Neuron* **9**: 955–966.
9. Kirshenbaum, LA, Abdellatif, M, Chakraborty, S and Schneider, MD (1996). Human E2F-1 reactivates cell cycle progression in ventricular myocytes and represses cardiac gene transcription. *Dev Biol* **179**: 402–411.
10. Endo, T and Nadal-Ginard, B (1998). Reversal of myogenic terminal differentiation by SV40 large T antigen results in mitosis and apoptosis. *J Cell Sci* **111 (Pt 8)**: 1081–1093.
11. Latella, L, Sacco, A, Pajalunga, D, Tiainen, M, Macera, D, D'Angelo, M *et al.* (2001). Reconstitution of cyclin D1-associated kinase activity drives terminally differentiated cells into the cell cycle. *Mol Cell Biol* **21**: 5631–5643.
12. Campa, VM, Gutiérrez-Lanza, R, Cerignoli, F, Díaz-Trelles, R, Nelson, B, Tsuji, T *et al.* (2008). Notch activates cell cycle reentry and progression in quiescent cardiomyocytes. *J Cell Biol* **183**: 129–141.
13. Sulg, M, Kirjavainen, A, Pajusola, K, Bueler, H, Ylikoski, J, Laiho, M *et al.* (2010). Differential sensitivity of the inner ear sensory cell populations to forced cell cycle re-entry and p53 induction. *J Neurochem* **112**: 1513–1526.
14. Pajalunga, D, Puggioni, EM, Mazzola, A, Leva, V, Montecucco, A and Crescenzi, M (2010). DNA replication is intrinsically hindered in terminally differentiated myotubes. *PLoS One* **5**: e11559.
15. Gonçalves, MA (2005). Adeno-associated virus: from defective virus to effective vector. *Virol J* **2**: 43.
16. Van Vliet, E, Melis, M, Foidart, JM and Van Ewijk, W (1986). Reticular fibroblasts in peripheral lymphoid organs identified by a monoclonal antibody. *J Histochem Cytochem* **34**: 883–890.
17. Musarò, A, McCullagh, K, Paul, A, Houghton, L, Dobrowolny, G, Molinaro, M *et al.* (2001). Localized Igf-1 transgene expression sustains hypertrophy and regeneration in senescent skeletal muscle. *Nat Genet* **27**: 195–200.
18. Lescaudron, L, Creuzet, SE, Li, Z, Paulin, D and Fontaine-Pérus, J (1997). Desmin-lacZ transgene expression and regeneration within skeletal muscle transplants. *J Muscle Res Cell Motil* **18**: 631–641.
19. Dey, BK, Gagan, J, Yan, Z and Dutta, A (2012). miR-26a is required for skeletal muscle differentiation and regeneration in mice. *Genes Dev* **26**: 2180–2191.
20. Cmielová, J and Rezáčová, M (2011). p21Cip1/Waf1 protein and its function based on a subcellular localization [corrected]. *J Cell Biochem* **112**: 3502–3506.
21. Rogakou, EP, Boon, C, Redon, C and Bonner, WM (1999). Megabase chromatin domains involved in DNA double-strand breaks in vivo. *J Cell Biol* **146**: 905–916.
22. Hawke, TJ, Meeson, AP, Jiang, N, Graham, S, Hutcheson, K, DiMaio, JM *et al.* (2003). p21 is essential for normal myogenic progenitor cell function in regenerating skeletal muscle. *Am J Physiol Cell Physiol* **285**: C1019–C1027.
23. Chakkalakal, JV, Christensen, J, Xiang, W, Tierney, MT, Boscolo, FS, Sacco, A *et al.* (2014). Early forming label-retaining muscle stem cells require p27kip1 for maintenance of the primitive state. *Development* **141**: 1649–1659.
24. Barbaric, I, Miller, G and Dear, TN (2007). Appearances can be deceiving: phenotypes of knockout mice. *Brief Funct Genomic Proteomic* **6**: 91–103.
25. Camarda, G, Siepi, F, Pajalunga, D, Bernardini, C, Rossi, R, Montecucco, A *et al.* (2004). A pRb-independent mechanism preserves the postmitotic state in terminally differentiated skeletal muscle cells. *J Cell Biol* **167**: 417–423.
26. Donà, M, Sandri, M, Rossini, K, Dell'Aica, I, Podhorska-Okolow, M and Carraro, U (2003). Functional *in vivo* gene transfer into the myofibers of adult skeletal muscle. *Biochem Biophys Res Commun* **312**: 1132–1138.

27. Arsic, N, Zentilin, L, Zacchigna, S, Santoro, D, Stanta, G, Salvi, A *et al.* (2003). Induction of functional neovascularization by combined VEGF and angiopoietin-1 gene transfer using AAV vectors. *Mol Ther* **7**: 450–459.
28. Tessitore, A, Parisi, F, Denti, MA, Allocca, M, Di Vicino, U, Domenici, L *et al.* (2006). Preferential silencing of a common dominant rhodopsin mutation does not inhibit retinal degeneration in a transgenic model. *Mol Ther* **14**: 692–699.
29. Rosenblatt, JD, Lunt, AI, Parry, DJ and Partridge, TA (1995). Culturing satellite cells from living single muscle fiber explants. *In Vitro Cell Dev Biol Anim* **31**: 773–779.
30. Bader, D, Masakiò, T and Fischman, DA (1982). Immunochemical analysis of myosin heavy chain during avian myogenesis in vivo and in vitro. *J Cell Biol* **95**: 763–770.
31. Fasanaro, P, Magenta, A, Zaccagnini, G, Cicchillitti, L, Fucile, S, Eusebi, F *et al.* (2006). Cyclin D1 degradation enhances endothelial cell survival upon oxidative stress. *FASEB J* **20**: 1242–1244.
32. Rando, TA and Blau, HM (1994). Primary mouse myoblast purification, characterization, and transplantation for cell-mediated gene therapy. *J Cell Biol* **125**: 1275–1287.
33. Del Prete, Z, Musarò, A and Rizzuto, E (2008). Measuring mechanical properties, including isotonic fatigue, of fast and slow MLC/mIgf-1 transgenic skeletal muscle. *Ann Biomed Eng* **36**: 1281–1290.
34. Tice, RR, Agurell, E, Anderson, D, Burlinson, B, Hartmann, A, Kobayashi *et al.* (2000). Single cell gel/comet assay: guidelines for in vitro and in vivo genetic toxicology testing. *Environmental and Molecular Mutagenesis* **35**: 206–221.
35. Musio, A, Marrella, V, Sobacchi, C, Rucci, F, Fariselli, L, Giliani, S *et al.* (2005). Damaging-agent sensitivity of Artemis-deficient cell lines. *Eur J Immunol* **35**: 1250–1256.
36. Kolman, A, Kotova, N and Grawé, J (2002). Aphidicolin induces 6-thioguanine resistant mutants in human diploid fibroblasts. *Mutat Res* **499**: 227–233.